Real-time GPS seismology with a stand-alone receiver: A preliminary feasibility demonstration

G. Colosimo,[1] M. Crespi,[1] and A. Mazzoni[1]

Received 20 August 2010; revised 25 June 2011; accepted 19 August 2011; published 3 November 2011.

[1] We show the feasibility of a real-time estimation of waveforms and coseismic displacements, within a few centimeters in accuracy, with a stand-alone dual-frequency Global Positioning System (GPS) receiver using a so-called "variometric" approach. The approach is based on time single-differences of carrier phase observations collected at a high-rate (1 Hz or more) using a stand-alone receiver, and on standard GPS broadcast products (orbits and clocks), which are ancillary information routinely available in real time. In the approach, first, the time series of epoch-by-epoch displacements are estimated. Then, provided that the collected observations are continuous, they can be summed over the interval (limited to a few minutes) over which an earthquake occurs. Since epoch-by-epoch displacements divided by the interval between consecutive epochs are essentially equal to the epoch-by-epoch velocities, this is equivalent to saying that we are using the GPS receiver as a velocimeter. Estimation biases, due to the possible mismodeling of various intervening effects (such as multipath, residual clock errors, orbit errors, and atmospheric errors), accumulate over time and display their signature as a trend in coseismic displacements. The trend can be considered linear and easily removed, at least for short intervals. Since the proposed approach (named VADASE (Variometric Approach for Displacements Analysis Stand-alone Engine)) does not require either additional technological complexity or a centralized data analysis, in principle it can be embedded into GPS receiver firmware, thereby providing a significant contribution to tsunami warning and other hazard assessment systems. After a preliminary test using a simulated example, the effectiveness of this approach was proven using real data. We analyzed the 1 Hz GPS data recorded by the International Global Navigation Satellite Systems Service station BREW during the Denali Fault, Alaska, earthquake (Mw 7.9, 3 November, 2002, 22:12:41 UTC), as well as the 5 Hz data collected by some of the stations of the University NAVSTAR Consortium-Plate Boundary Observatory network and the California Real Time Network during the Baja California, Mexico, earthquake (Mw 7.2, 4 April, 2010, 22:40:42 UTC). Comparisons of the results obtained using VADASE, as well as other already well-established approaches, displayed agreement to within a few centimeters.

Citation: Colosimo, G., M. Crespi, and A. Mazzoni (2011), Real-time GPS seismology with a stand-alone receiver: A preliminary feasibility demonstration, *J. Geophys. Res.*, *116*, B11302, doi:10.1029/2010JB007941.

1. Introduction

1.1. The Processing Approaches Presently Used in GPS Seismology: Pros and Cons

[2] The Global Positioning System (GPS) has been widely used for two decades for estimating coseismic displacements, with accuracies ranging from a few millimeters to a few centimeters, in support of both the modeling of fault rupture and investigations of mechanical fault behavior. The seismic moment (and the moment magnitude (M_w)) can also be estimated without the problems of saturation that commonly influence seismometers close to large earthquakes [*Bock et al.*, 1993, 2000; *Kouba*, 2003; *Larson et al.*, 2003; *Bock et al.*, 2004; *Langbein and Bock*, 2004; *Kouba*, 2005; *Plag et al.*, 2005; *Blewitt et al.*, 2006; *Bock and Genrich*, 2006; *Larson et al.*, 2007; *Bilich et al.*, 2008; *Larson and Miyazaki*, 2008; *Miyazaki and Larson*, 2008; *Larson*, 2009; UNAVCO, Science Highlights 2010-UNAVCO Event Response to the Mw = 7.2 El Mayor-Cucapah Baja California, Mexico, Earthquake April 4, 2010, online article, 2010, http://www.unavco.org/research_science/science_highlights/2010/M7.2-Baja.html#Results].

[3] The following two approaches have been adopted for GPS seismology: single Precise Point Positioning [*Hofman-*

[1]DICEA–Area di Geodesia e Geomatica, Università di Roma "La Sapienza," Rome, Italy.

0148-0227/11/2010JB007941

Wellenhof et al., 2008, pp. 166–167] and differential positioning [*Hofman-Wellenhof et al.*, 2008, p. 169].

[4] Coseismic displacements have been estimated with a post-processing approach using various scientific software (Bernese, GAMIT, GIPSY), while employing high quality products (orbits, clocks, Earth Orientation Parameters (EOPs)) supplied by the International Global Navigation Satellite Systems (GNSS) Service (IGS) [*Dow et al.*, 2009] or by NASA's Jet Propulsion Laboratory (JPL). The products are freely available and have a latency period ranging from 17–41 h (rapid products) to 12–18 days (final products). Even at present, these products are not routinely available with the appropriate high quality in real time.

[5] Additionally, the long latency, which prevents real-time coseismic displacement estimations, has been overcome by the technique referred to as Instantaneous Positioning [*Bock et al.*, 2000]. The technique is based on differential positioning and allows the fundamental resolution of integer-cycle phase ambiguities [*Hofman-Wellenhof et al.*, 2008, p. 107] with a single epoch only for the dual-frequency phase [*Hofman-Wellenhof et al.*, 2008, p. 111] and pseudorange [*Hofman-Wellenhof et al.*, 2008, p. 105] data. Therefore, Instantaneous Positioning provides a precise independently computed position for each observational epoch, at the sampling rate of the receiver.

[6] Even if this technique is able to guarantee high, real-time accuracy (at 1 cm level), it only provides a relative coseismic displacement, which is the coseismic displacement with respect to (at least) one reference station due to the adopted differential positioning approach. Furthermore, in order to achieve the mentioned accuracy at 1 cm in real time, Instantaneous Positioning requires both a complex and a continuously linked infrastructure (GPS permanent network) with a maximum average inter-station distance of up to several tens to a few hundreds of kilometers. Common processing of collected data is performed in a centralized analysis center, a serious limitation for strong earthquakes which may involve the entire area covered by a GPS permanent network, including reference station(s). For such a case, coseismic displacements in the global reference frame are not available any more, since even the reference station(s) undergo(es) a displacement. On the other hand, for realistic natural hazard applications, one cannot assume a very large GPS permanent network since (a) far reference station(s) cause(s) a loss of accuracy in real-time differential positioning, and/or since economic considerations limit the number of stations that can be installed and managed together in a unique infrastructure.

[7] Overall, GPS seismology has been proven to be an effective tool, but requires either high quality products (orbits, clocks, EOPs) to obtain an a posteriori highest accuracy estimation of coseismic displacements within the global reference frame, or a complex and continuously linked infrastructure (GPS permanent network) in order to obtain real-time, highly accurate (at 1 cm level), but only relative, coseismic displacements.

1.2. The Present Challenges of Real-Time GPS Seismology and Our Proposal

[8] In considering that very high-rate (up to 100 Hz) GPS measurements are now commonly available, a new and important contribution of GPS seismology is real-time earthquake source determinations, which may also contribute to tsunami warning systems.

[9] In this regard, during the Real Time GPS Science Requirements Workshop held in September, 2007 in Leavenworth (Washington, USA) the goal of achieving 1 cm real-time GNSS coseismic displacement accuracies in the global reference frame, within the three minutes following an earthquake, was adopted [*Blewitt et al.*, 2009].

[10] Following this recommendation, we propose a new approach for estimating coseismic displacements in the global reference frame in real time. The approach is based on a single GPS station technique that is able to overcome some of the difficulties displayed by the two aforementioned, presently adopted, approaches for GPS Seismology.

[11] Our approach (named VADASE (Variometric Approach for Displacements Analysis Stand-alone Engine)) is based on a so-called "variometric" solution. The approach only requires the standard GPS broadcast products (orbits and clocks) and the observations collected by a unique, stand-alone, dual-frequency GPS receiver.

[12] Since VADASE does not require either additional technological complexity or a centralized data analysis, in principle it can be embedded into the GPS receiver firmware, thereby providing a significant contribution to tsunami warning systems.

[13] In section 2 the basic ideas behind VADASE and the related estimation model are introduced. In section 3 VADASE is applied to a simulated example. For this work two solutions were computed and compared. Both solutions were obtained using the same GPS observations. The first solution utilizes standard GPS broadcast products (orbits and clocks) available in real time, while the second utilizes the best quality products (orbits and clocks, EOPs) supplied by IGS, a posteriori. The results indicate that even GPS broadcast products (orbits and clocks) are suitable for fully exploiting the potential of the variometric approach for detecting 3D displacements that have occurred during the interval between two consecutive measurement epochs, at centimeter level accuracy. Since the displacement divided by its occurring interval is essentially equal to a velocity, this is equivalent to saying that we are using the GPS receiver as a velocimeter.

[14] In section 4 our approach is applied a posteriori to real-life examples, again using GPS broadcast products as well as IGS best quality products. In regard to reconstructing waveforms and coseismic displacements, below we discuss the possibility of integrating the estimated velocity over intervals spanning a few minutes, while pointing out various problems (e.g., mismodeling and data continuity). We also compare our results to others obtained from well-known approaches (i.e., Precise Point Positioning and Instantaneous Positioning).

[15] In section 5 a simplification of the VADASE estimation model is presented, taking into consideration the outcomes introduced in section 3; the same accuracy level is achieved. Finally, in section 6, we draw a few conclusions and discuss future research directions.

2. The Variometric Approach and Its Estimation Model

[16] In this section we present the basic idea of VADASE and the related estimation model. We begin by introducing the standard raw carrier phase observation equation

[*Hofman-Wellenhof et al.*, 2008, pp. 107, 118, 128, 141, 154], which in length units reads

$$\lambda\Phi^s_r = \rho^s_r + c(\delta t_r - \delta t^s) + T^s_r - I^s_r - \lambda N^s_r + p^s_r + m^s_r + \varepsilon^s_r \quad (1)$$

where subscript (r) refers to a particular receiver and superscript (s) to a satellite. $\Phi^s{}_r$ is the carrier phase observation of the receiver with respect to the satellite; λ is the carrier phase wavelength; $\rho^s{}_r$ is the geometric range (i.e., the distance between the satellite and the receiver); c is the speed of light; δt_r and δt^s are the receiver and the satellite clock errors, respectively; $T^s{}_r$ and $I^s{}_r$ are the tropospheric and the ionospheric delays along the path from the satellite to the receiver, respectively; $N^s{}_r$ is the initial phase ambiguity; $p^s{}_r$ is the sum of the other effects (relativistic effects, phase center variations, phase wind-up [*Hofman-Wellenhof et al.*, 2008, p. 145]); and $m^s{}_r$ and $\varepsilon^s{}_r$ represent the multipath and the noise, respectively.

[17] If we consider dual frequency GPS observations free from cycle slips [*Hofman-Wellenhof et al.*, 2008, pp. 194–195] and if we differentiate equation (1) in the time between two consecutive epochs ($t, t+1$), the ionospheric term may be canceled to the second order by applying the ionosphere-free combination [*Hofman-Wellenhof et al.*, 2008, pp. 127–128] to the time single-difference, which becomes the ionosphere-free time single-difference observation equation

$$\begin{aligned}\alpha\left[\lambda\Delta\Phi^s_r(t,t+1)\right]_{L1} + \beta\left[\lambda\Delta\Phi^s_r(t,t+1)\right]_{L2} \\ = \Delta\rho^s r(t,t+1) + c(\Delta\delta t_r(t,t+1) - \Delta\delta t^s(t,t+1)) \\ + \Delta T^s_r(t,t+1) + \Delta p^s_r(t,t+1) + \Delta m^s_r(t,t+1) \\ + \Delta\varepsilon^s_r(t,t+1)\end{aligned} \quad (2)$$

where $\alpha = (f^2{}_{L1}/(f^2{}_{L1}-f^2{}_{L2}))$ and $\beta = (-f^2{}_{L2}/(f^2{}_{L1}-f^2{}_{L2}))$ are the standard coefficients of the ionosphere-free combination, $\Delta m^s{}_r(t, t+1)$ and $\Delta\varepsilon^s{}_r(t, t+1)$ are the multipath and the noise in the time single-difference, respectively (note that while using this convention the value of t is always an integer and represents the time of the observation in units equal to the inverse of the observation collection rate).

[18] At first, if we hypothesize that the receiver is fixed in an Earth Centred Earth Fixed (ECEF) reference frame, the term $\Delta\rho^s{}_r(t, t+1)$ depends upon the change of the geometric range due to the satellite's orbital motion and the Earth's rotation ($[\Delta\rho^s{}_r(t, t+1)]_{OR}$). However, it is also dependent on the variation of the solid Earth tide and ocean loading ($[\Delta\rho^s{}_r(t, t+1)]_{EtOl}$) [*McCarthy and Petit*, 2004], so that

$$\Delta\rho^s_r(t,t+1) = \left[\Delta\rho^s_r(t,t+1)\right]_{OR} + \left[\Delta\rho^s_r(t,t+1)\right]_{EtOl} \quad (3)$$

On the other hand, if we hypothesize that the receiver underwent a 3D displacement $\Delta\xi_r(t, t+1)$ in an ECEF reference frame during the interval $(t, t+1)$, the term $\Delta\rho^s{}_r(t, t+1)$ also includes the effect of $\Delta\xi_r$ projected along the line-of-sight, which is approximately the same for the two consecutive epochs (t and $t+1$) if high-rate (≥1 Hz) observations are utilized. Therefore, we can write

$$\begin{aligned}\Delta\rho^s_r(t,t+1) &= \left[\Delta\rho^s_r(t,t+1)\right]_{OR} + \left[\Delta\rho^s_r(t,t+1)\right]_{EtOl} \\ &\quad + \left[\Delta\rho^s_r(t,t+1)\right]_{D} \\ &= \left[\Delta\rho^s_r(t,t+1)\right]_{OR} + \left[\Delta\rho^s_r(t,t+1)\right]_{EtOl} \\ &\quad + e^s_r \bullet \Delta\xi_r(t,t+1)\end{aligned} \quad (4)$$

where $\boldsymbol{e}^s_{\boldsymbol{r}}$ is the unit vector from the satellite to the receiver at epoch t, and the symbol • indicates the scalar product between the vectors $\boldsymbol{e}^s_{\boldsymbol{r}}$ and $\Delta\xi_r(t, t+1)$.

[19] Here, it should be suddenly noted that the displacement $\Delta\xi_r(t, t+1)$, if divided by the interval between consecutive epochs ($t, t+1$), is equal to the (mean) velocity over the interval $(t, t+1)$ itself. Therefore, the displacement, $\Delta\xi_r(t, t+1)$, which is expressed in units of length, is basically equivalent to a velocity, and we refer to it as the "velocity" in the following discussion. Overall, we can summarize this remark just saying that we are basically using the GPS receiver as a velocimeter.

[20] The tropospheric term, $\Delta T^s{}_r(t, t+1)$, represents the variation of tropospheric delay during the interval $(t, t+1)$, and is modeled, here, by computing the Tropospheric Zenith Delay (TZD_{SB}) according to the Saastamoinen model [*Saastamoinen*, 1972] using a standard atmosphere [*Berg*, 1948] and by applying the simple inverse cosine ($1/\cos(Z)$) mapping function, as follows:

$$\Delta T^s_r(t,t+1) = TZD_{SB}\left[1/\cos\left(Z^s_r(t+1)\right) - 1/\cos\left(Z^s_r(t)\right)\right] \quad (5)$$

where $Z^s{}_r$ is the zenith angle of the satellite (s) with respect to the receiver (r).

[21] If we introduce equations (4) and (5) into equation (2) and simplify the notation by omitting the epochs ($t, t+1$) indication, we obtain

$$\begin{aligned}\alpha\left[\lambda\Delta\Phi^s_r\right]_{L1} + \beta\left[\lambda\Delta\Phi^s_r\right]_{L2} \\ = \left[\Delta\rho^s_r\right]_{OR} + \left[\Delta\rho^s_r\right]_{EtOl} + \boldsymbol{e}^s_{\boldsymbol{r}} \bullet \Delta\xi_{\boldsymbol{r}} + c(\Delta\delta t_r - \Delta\delta t^s) \\ + TZD_{SB}\left[1/\cos\left(Z^s_r(t+1)\right) - 1/\cos\left(Z^s_r(t)\right)\right] + \Delta p^s_r \\ + \Delta m^s_r + \Delta\varepsilon^s_r\end{aligned} \quad (6)$$

which we can be rewritten in the form of the so defined variometric equation, as follows:

$$\begin{aligned}\alpha\left[\lambda\Delta\Phi^s_r\right]_{L1} + \beta\left[\lambda\Delta\Phi^s_r\right]_{L2} \\ = \left(\boldsymbol{e}^s_{\boldsymbol{r}} \bullet \Delta\xi_r + c\Delta\delta t_r\right) + \Big(\left[\Delta\rho^s_r\right]_{OR} - c\Delta\delta t^s \\ + TZD_{SB}\left[1/\cos\left(Z^s_r(t+1)\right) - 1/\cos\left(Z^s_r(t)\right)\right]\Big) \\ + \Big(\left[\Delta\rho^s_r\right]_{EtOl} + \Delta p^s_r\Big) + \Delta m^s_r + \Delta\varepsilon^s_r\end{aligned} \quad (7)$$

where $\alpha[\lambda\Delta\Phi^s{}_r]_{L1} + \beta[\lambda\Delta\Phi^s{}_r]_{L2}$ are the time single-difference ionosphere-free observations; $(\boldsymbol{e}^s_{\boldsymbol{r}} \bullet \Delta\xi_{\boldsymbol{r}} + c\Delta\delta t_r)$ are terms containing the four unknown parameters (the 3D velocity $\Delta\xi_{\boldsymbol{r}}$, and the receiver clock error variation $\Delta\delta t_r$); $([\Delta\rho^s{}_r]_{OR} - c\Delta\delta t^s + TZD_{SB}\,[1/\cos(Z^s{}_r(t+1)) - 1/\cos(Z^s{}_r(t))])$ is the largest part of the known term that can be computed on the basis of known orbits and clocks and for the chosen tropospheric model; $([\Delta\rho^s{}_r]_{EtOl} + \Delta p^s{}_r)$ is an additional much smaller known term that can be computed with proper models for all of the considered effects; and $\Delta m^s{}_r$ and $\Delta\varepsilon^s{}_r$ are the multipath and noise terms, as described previously.

[22] Equation (7) represents the functional model of the least squares estimation problem. Well known is that low elevation observations are usually noisier, such that the observations are weighted by the squared cosine of the satellite zenith angle (Z) [*Dach et al.*, 2007, p. 144], as follows:

$$w = \cos^2(Z) \quad (8)$$

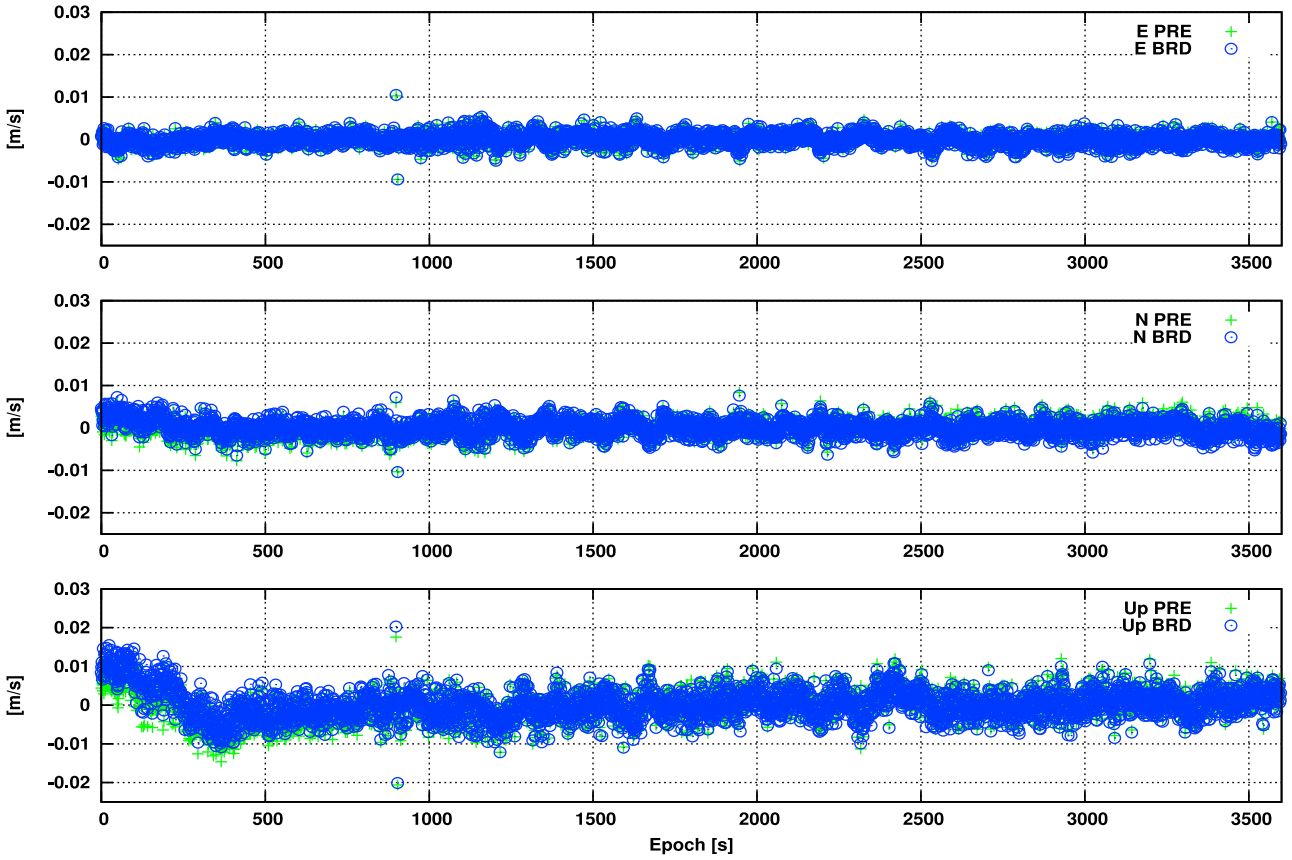

Figure 1. M0SE estimated 3D velocities using GPS broadcast products (orbits and clocks) available in real time (BRD solution), and the best quality products (orbits and clocks) supplied by IGS a posteriori (PRE solution) in the 1 h interval 04:00:00–04:59:59 on 20 February 2010, GPS time.

The least squares estimation of the 3D velocities is based upon the entire set of variometric equations (7), which can be written for two generic consecutive epochs (t and $t + 1$). The number of variometric equations obviously depends on the number of satellites common to the two epochs, and at least four satellites are obviously necessary in order to estimate the four unknown parameters (the 3D velocity $\Delta\xi_r$, and the receiver clock error variation $\Delta\delta t_r$) for each consecutive epoch couple.

[23] Here, it is useful to note that we can relax the hypothesis of dual frequency observations free from cycle slips. In fact, as for the Instantaneous Positioning strategy [*Bock et al.*, 2000], the losses of lock and cycle slips can be easily recognized during the analysis of the time series of the estimated 3D velocities $\Delta\xi_r$. The corresponding epochs can be rejected by setting a suitable threshold.

[24] A position-based modified real-time sidereal filtering, as proposed by *Choi et al.* [2004] could be used to mitigate the multipath $\Delta m^s{}_r$; however, at present this effect is neglected.

3. The Application of the Variometric Approach to a Simulated Example

[25] The effectiveness of the presented variometric approach was proven by implementing a suited software that, at first, was applied to the simulated example, as described below. The main goal of this first test was to show the potential of VADASE for estimating the velocities $\Delta\xi_r$ related to two consecutive measurement epochs (t and $t + 1$) using even GPS broadcast products (orbits and clocks).

[26] We began by considering the actual stream of carrier phase observations (file REALM0SE) collected at a rate of 1 Hz by the M0SE GPS permanent station (Rome, Italy) in the interval from 04:00:00 to 04:59:59, 20 February 2010. In order to introduce the effect of a known displacement into these observations, the simulation tool that is included as a part of the Bernese software (v. 5.0) [*Dach et al.*, 2007, p. 347] was utilized. The tool is able to simulate GPS observations that can be collected at a certain location under certain satellite scenarios (orbits, clocks, EOPs) and to hypothesize a certain error model.

[27] We first generated the error-free carrier phase observations by fixing the position of M0SE to its known ITRF2005 coordinates and by using the IGS precise products (orbits, clocks and EOPs) for the interval from 04:00:00–04:59:59, 20 February 2010, as a satellite scenario (file SIMUM0SE).

[28] Next, we generated error-free carrier phase observations by referring to a position of M0SE that was shifted 1 cm to the East and to the North, and 2 cm up with respect to ITRF2005 coordinates, using the same satellite scenario and procedure for the same interval as considered previously (file SIMUM0SE-SHFT).

Table 1. M0SE Estimated Velocities Versus Imposed Displacements[a]

Epoch	Direction	Expected Velocity	Estimated Velocity PRE	Estimated Velocity BRD
899	E [m/s]	0.0100	0.0103	0.0105
	N [m/s]	0.0100	0.0060	0.0072
	Up [m/s]	0.0200	0.0176	0.0203
904	E [m/s]	−0.0100	−0.0094	−0.0094
	N [m/s]	−0.0100	−0.0103	−0.0104
	Up [m/s]	−0.0200	−0.0206	−0.0201

[a]M0SE comparisons between imposed displacements and estimated 3D velocities using GPS broadcast products (orbits and clocks) available in real time (BRD solution) and the best quality products (orbits and clocks) supplied by IGS a posteriori (PRE solution) at epochs 899–900 and 904–905 of the 1 h interval, 04:00:00–04:59:59, 20 February 2010, GPS time.

[29] Therefore, the differences (file DIFFM0SE equal to file SIMUM0SE-SHFT minus file SIMUM0SE) between the corresponding (same epoch, same satellite, same frequency) error-free carrier phase observations represent the error-free effect of the synthetically imposed (East, North, and up) 3D displacements (1 cm, 1 cm, and 2 cm, respectively) on the carrier phase observations themselves.

[30] Finally, by assuming that a 3D displacement from the ITRF2005 position to the shifted position occurred at epoch 900 and that the displacement to the original ITRF2005 position occurred at epoch 905 (assuming epoch 0 at 04:00:00, 20 February 2010) we summed the mentioned difference values (file DIFFM0SE) from epoch 900 to epoch 905 to *actual* carrier phase observations (file REALM0SE). In this way, we generated a stream of carrier phase observations (file REALM0SE-SHFT) that were impacted by the real noise *and* that included the effect of the imposed 3D displacements from epoch 900 to epoch 905.

[31] We tested the variometric approach on this data stream by looking for the imposed displacements, which caused a 3D velocity $\Delta\xi_r$ from epoch 899 to epoch 900 and the 3D opposite velocity from epoch 904 to epoch 905, when the original ITRF2005 position is recovered.

[32] Our results were quite encouraging, since the East, North, and up displacements of +1 cm, +1 cm, and +2 cm, respectively, at epoch 900; and of −1 cm, −1 cm, and −2 cm, respectively, at epoch 905 were clearly visible in the time

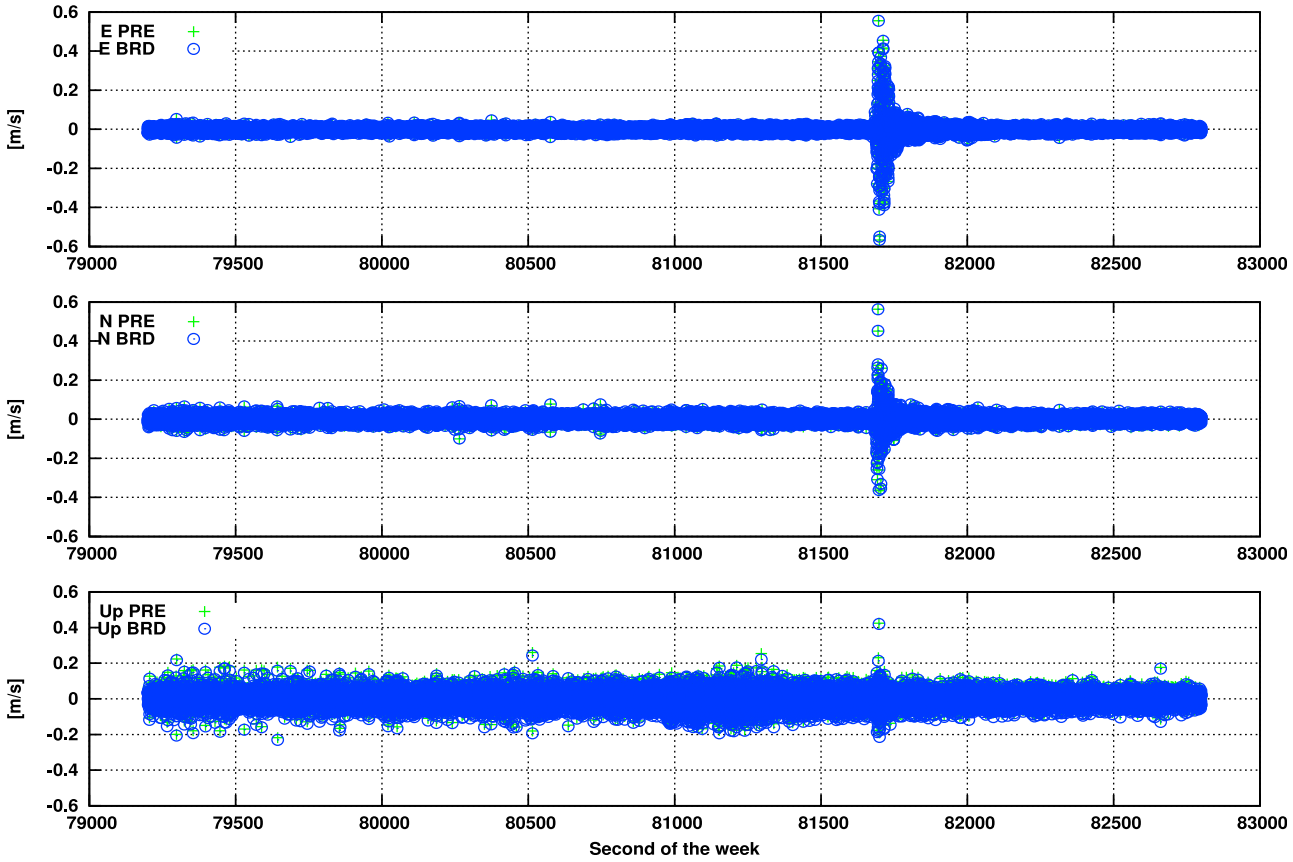

Figure 2. P496 estimated 3D velocities using GPS broadcast products (orbits and clocks) available in real time (BRD solution), and the best quality products (orbits and clocks) supplied by IGS a posteriori (PRE solution) in the 1 h interval 22:00:00–23:00:00 on 4 April 2010, GPS time.

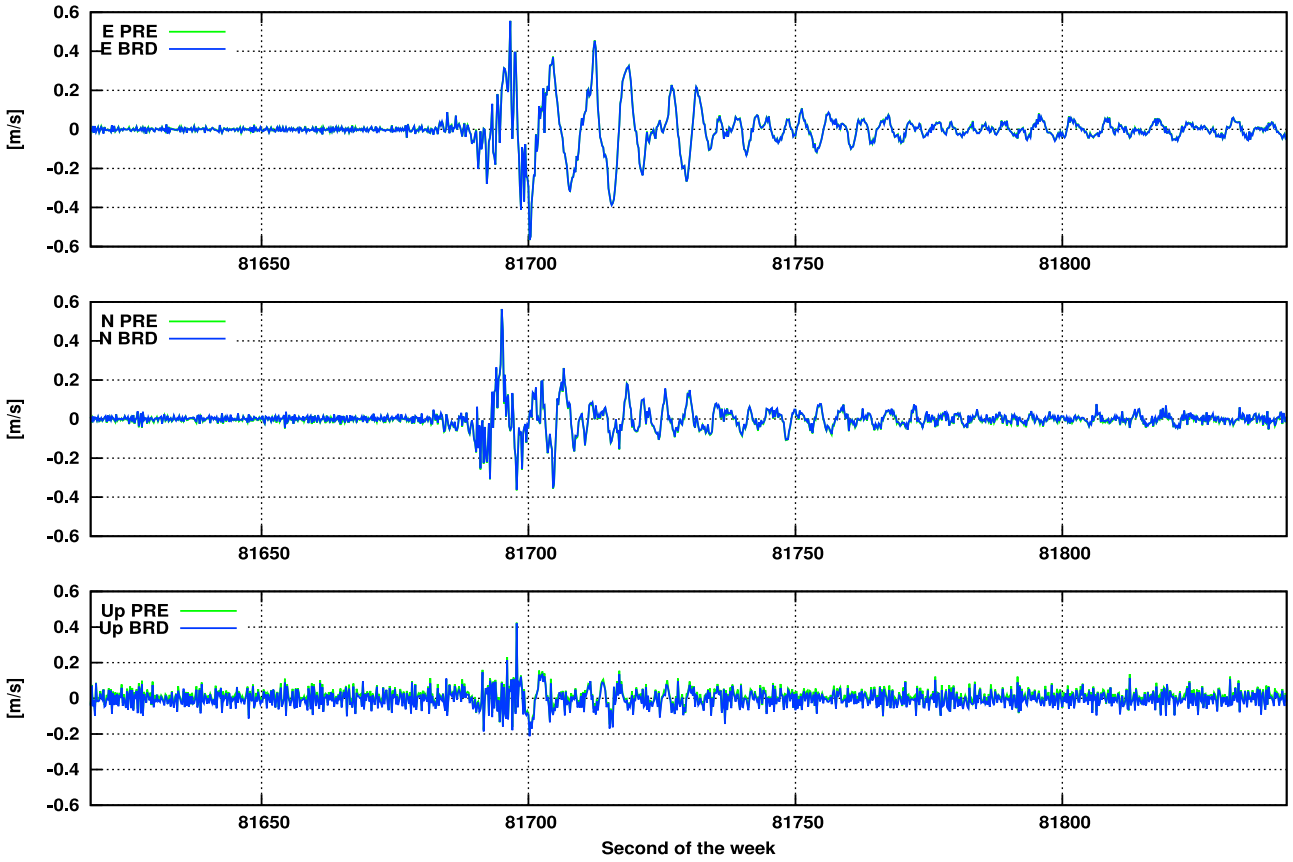

Figure 3. P496 estimated 3D velocities using GPS broadcast products (orbits and clocks) available in real time (BRD solution), and the best quality products (orbits and clocks) supplied by IGS a posteriori (PRE solution) in the 220 s interval 22:40:20–22:44:00 on 4 April 2010, GPS time.

series of the 3D velocities $\Delta\xi_r$. Displacements were estimated with an accuracy of 1–2 mm/s in both the horizontal and up directions by using the GPS broadcast products (orbits and clocks) available in real time (BRD solution) and the best quality products (orbits and clocks) supplied by IGS, a posteriori (PRE solution) (Figure 1, Table 1).

[33] In addition, we evaluated the global agreement between the BRD and PRE solutions in terms of the standard deviation of 3D velocity differences over the 1 h interval, 04:00:00–04:59:59, 20 February 2010. The agreement was within 1 mm/s for the horizontal coordinates and 2 mm/s for the height.

4. The Application of the Variometric Approach to Real Data: Waveforms and Coseismic Displacement Estimations, and a Comparison With Other Strategies

4.1. Velocity Estimations

[34] In order to assess the potential for estimating 3D velocities $\Delta\xi_r$ due to an earthquake, the variometric approach was applied to the 5 Hz data collected by the University NAVSTAR Consortium-Plate Boundary Observatory (UNAVCO-PBO) station P496 during the Baja California, Mexico earthquake (Mw 7.2, 4 April 2010, 22:40:42 UTC; GPS Time–UTC = 15 s).

[35] Again, the earthquake signature was clearly evident in the 1 h interval time series of the 3D velocities $\Delta\xi_r$, as estimated using both the GPS broadcast products (BRD solution) and the best quality products supplied by IGS (PRE solution) (Figure 2). When we zoomed in on the 220 s interval from 22:40:20 to 22:44:00, 4 April 2010, GPS time when earthquake waves arrived (Figure 3), the agreement between the BRD and the PRE solutions (in terms of the standard deviations of the 3D velocity differences) was again within 5 mm/s in the horizontal and within 10 mm/s in height (Table 2). Therefore, the variometric approach again appeared effective for estimating real-time 3D velocities $\Delta\xi_r$ due to an earthquake.

4.2. Coseismic Displacement Estimations

[36] We were then faced with the problem of reconstructing waveforms and coseismic displacements corresponding to estimated 3D velocities $\Delta\xi_r$ in the global reference frame.

[37] To this aim, provided that continuous data have been acquired, we have to integrate the time series of these velocities over an interval in order to reconstruct the occurring receiver motion, which is the coseismic displacement. Well known is that this (discrete) integration is very sensitive to estimation biases due to the possible mismodeling of different intervening effects (such as multipath,

Table 2. P496–PRE Versus BRD Estimated 3D Velocities[a]

	BRD – PRE [m/s]
E	0.0020
N	0.0025
Up	0.0080

[a]P496 comparisons between estimated 3D velocities using GPS broadcast products (orbits and clocks) available in real-time (BRD solution) and the best quality products (orbits and clocks) supplied by IGS a posteriori (PRE solution); 220 s interval, 22:40:20–22:44:00, 4 April 2010, GPS time.

residual clock errors, orbit errors, and atmospheric errors) that accumulate over time and display their signature as a trend in the coseismic displacements themselves.

[38] In regard to a possible strategy for trend removal, and in considering the goal of this work; that is, to estimate waveforms and coseismic displacements in the global reference frame in real time when an earthquake occurs, we first decided to limit the integration interval to five minutes, which can be assumed as reasonable even for quite strong earthquakes. Thanks to this limitation, we hypothesize that the trend may be considered linear for this interval; here, the reader should note that a linear trend in coseismic displacements corresponds to a constant bias in the time series of the 3D velocities $\Delta\xi_r$.

[39] We also assume that this bias may be estimated over the 1 min interval prior to the earthquake and removed from the estimated 3D velocities for the duration of the entire earthquake. In this respect, here, it should be recognized that we cannot estimate the bias by considering the time series of the estimated 3D velocities $\Delta\xi_r$ during the duration of the entire earthquake. In fact, for this case the effect of a possible global displacement due to the earthquake would be wrongly included in the estimation.

[40] In order to check the effectiveness of the proposed strategy for trend removal the same type of data, collected by the UNAVCO-PBO station P496, were analyzed. The solutions obtained using GPS broadcast products (BRD solution) and the best quality products supplied by IGS (PRE solution) clearly displayed different trends (Figure 4, dashed lines), which were then removed, as described above. Following trend removals, the PRE and BRD solutions agreed within 1 mm in the horizontal and within 2 mm in height, in terms of the standard deviation of the differences (Figure 4, continuous lines).

4.3. Other Examples With Real Data

[41] The above described procedure for reconstructing waveforms and coseismic displacements was applied to the 5 Hz data collected by the UNAVCO-PBO stations P494

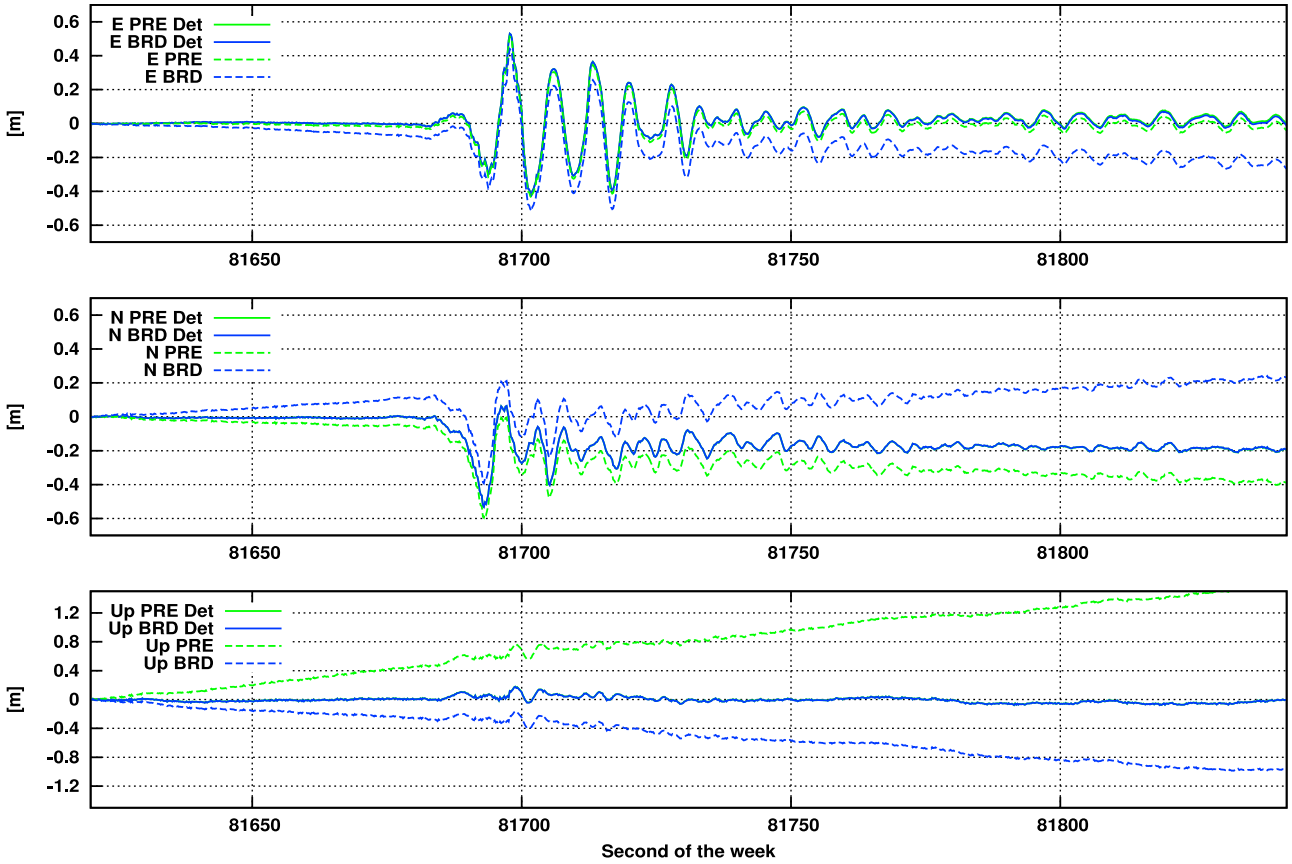

Figure 4. P496 coseismic displacements obtained by integrating the estimated 3D velocities using broadcast products (BRD solution), and the best quality products supplied by IGS (PRE solution) before (dashed lines) and after (continuous lines) trend removal; 220 s interval 22:40:20–22:44:00 on 4 April 2010, GPS time.

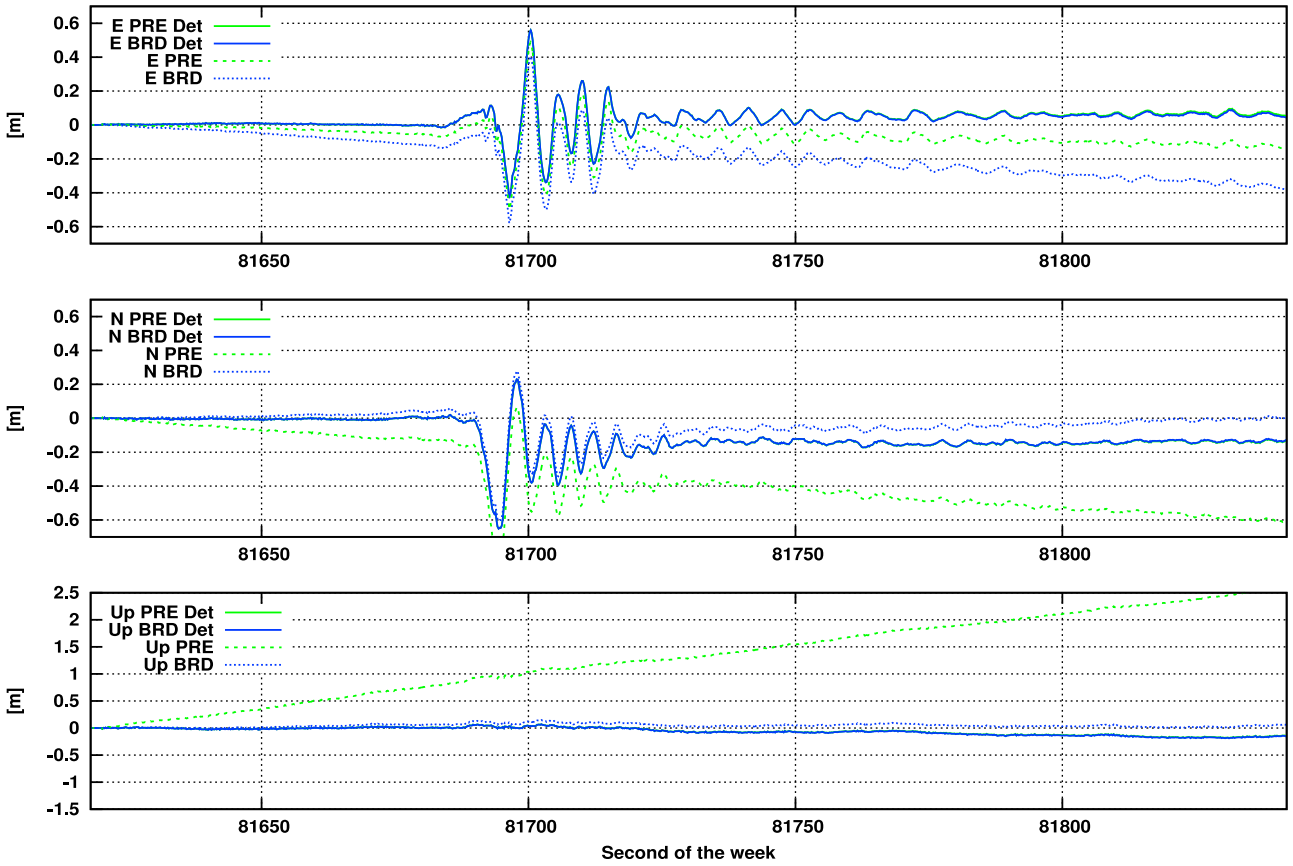

Figure 5. P494 coseismic displacements obtained by integrating the estimated 3D velocities using broadcast products (BRD solution), and the best quality products supplied by IGS (PRE solution) before (dashed lines) and after (continuous lines) trend removal; 220 s interval 22:40:20–22:44:00 on 4 April 2010, GPS time.

and P744 during the same Baja California, Mexico earthquake, and to the 1 Hz data collected by the IGS station BREW during the Denali Fault, Alaska earthquake (Mw 7.9, 3 November 2002, 22:12:41 UTC; GPS Time–UTC = 13 s). The data were chosen because they were publicly available along with the solutions obtained using different strategies (for example, Precise Point Positioning and Instantaneous Positioning strategies) [*Kouba*, 2003, UNAVCO, online article, 2010].

[42] The waveforms and coseismic displacements recovered with VADASE, by applying the described detrending, behaved similarly if the GPS broadcast products (BRD solution) and the best quality products supplied by IGS (PRE solution) were utilized (Figures 5, 6, and 7). Small differences after detrending that expanded to 2–3 cm at the end of the chosen integration interval were only found in the BREW solutions.

[43] As a result of substantial equivalence after trend removal of the PRE and BRD solutions to within a few centimeters, and by recalling that we were interested in the real-time solutions that were available for a stand-alone dual-frequency GPS receiver, only the BRD detrended coseismic displacements were compared with already well-established approaches.

[44] Using just a visual comparison with the solutions presented by UNAVCO (online article, 2010) (Figures 8 and 9) and *Kouba* [2003] (Figure 7) for the Baja California and the Denali Fault earthquakes, respectively, a high agreement both in the horizontal and the vertical (available for BREW only) components, at the level of a few centimeters was determined (if the waveform minima and maxima are considered).

5. The Simplified Variometric Estimation Model and Its Effectiveness

[45] In the end, we investigated the possibility of simplifying the variometric model (7) by neglecting a few of the terms. Until this point, by summarizing previous results obtained using the complete variometric model (7), we learned the following.

[46] 1. Discrete integration of 3D estimated velocities may be impacted by a trend, which we assumed to be linear if the integration interval was limited up to five minutes and had to be removed for any case.

[47] 2. Differences in recovering waveforms and coseismic displacements up to a few centimeters were seen if the GPS broadcast products (BRD solution) and the best quality products supplied by IGS (PRE solution) were used, such that GPS broadcast products, available in real time, were perfectly suited for our goal.

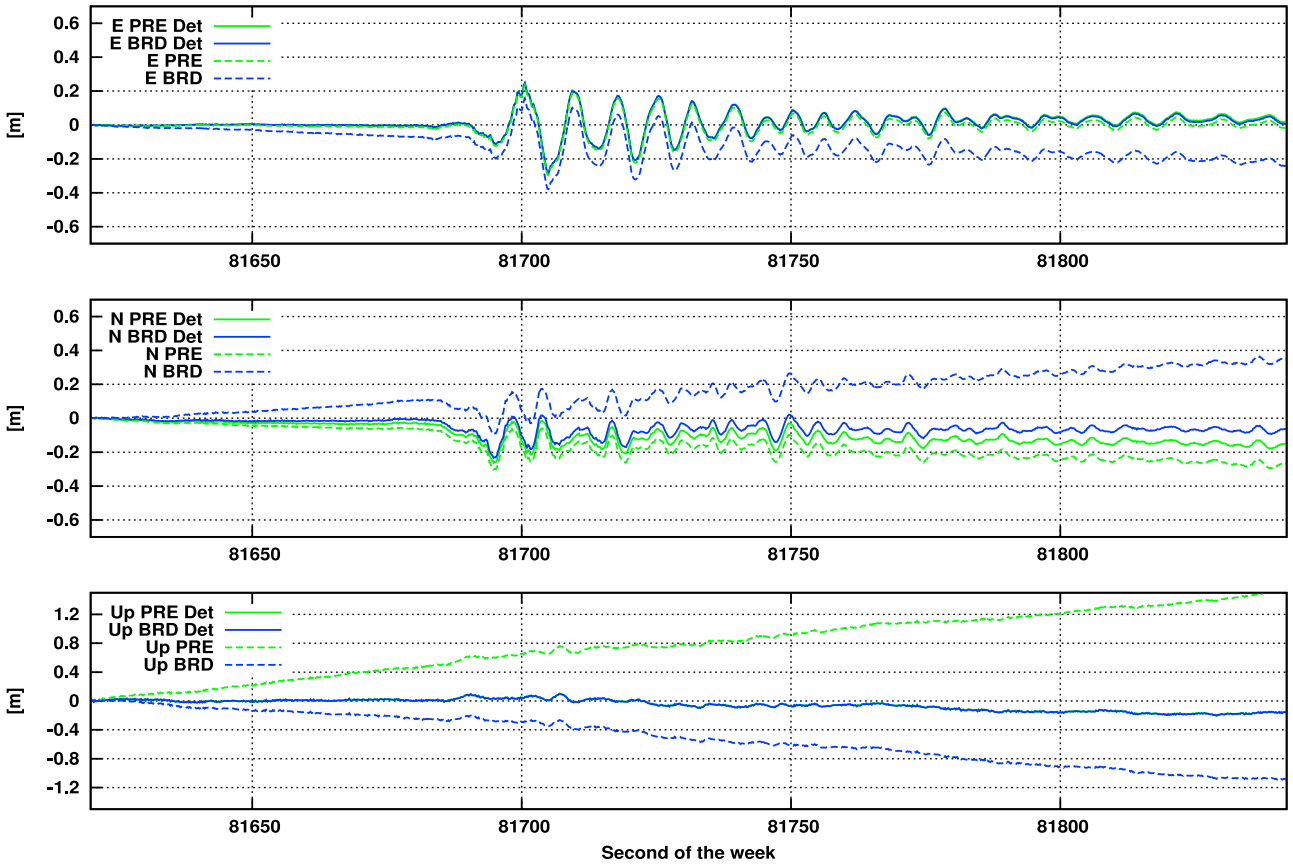

Figure 6. P744 coseismic displacements obtained by integrating the estimated 3D velocities using broadcast products (BRD solution), and the best quality products supplied by IGS (PRE solution) before (dashed lines) and after (continuous lines) trend removal; 220 s interval 22:40:20–22:44:00 on 4 April 2010, GPS time.

[48] By starting again from the standard raw carrier phase observation equation (1), here, we consider a one-frequency (suited for both L1 and L2 with proper wavelengths) simplified variometric equation, as follows:

$$\left[\lambda\Delta\Phi^s_r\right]_{L1,L2} = \left(e^s_r \bullet \Delta\xi_r + c\Delta\delta t_r\right) + \left(\left[\Delta\rho^s_r\right]_{OR} - c\Delta\delta t^s\right)_{BRD} + \Delta m^s_r + \Delta\varepsilon^s_r \quad (9)$$

where the effects due to the ionosphere, the troposphere, phase center variation, relativity, and phase wind-up were neglected. The term $([\Delta\rho^s{}_r]_{OR} - c\Delta\delta t^s)_{BRD}$ was computed using GPS broadcast products, and $\Delta m^s{}_r$ and $\Delta\varepsilon^s{}_r$ are the multipath (neglected as before) and the noise, respectively. Equation (9) represents the simplified functional model of the least squares estimation problem.

[49] In regard to the stochastic model, the same assumption as applied previously was utilized, and is now applied to both frequencies separately, as follows:

$$w\left(\left[\lambda\Delta\Phi^s_r\right]_{L1,L2}\right) = \cos^2(Z) \quad (10)$$

As before, the least squares estimation of 3D velocities is based upon the entire set of the variometric equation (9), which can be written (separately for L1 and L2) for two generic consecutive epochs (t and $t + 1$). The number of the simplified variometric equations obviously depends upon the number of satellites common to the two epochs, and at least four satellites are obviously necessary in order to estimate the four unknown parameters (the 3D velocity $\Delta\xi_r$, and the receiver clock error variation $\Delta\delta t_r$) for each consecutive epoch couple.

[50] Note that the simplified functional model (9) allows us to double the overall number of variometric equations and to open an investigation on the use of VADASE using single frequency receivers.

[51] The effectiveness of the simplified variometric model was proven by again considering the 5 Hz data collected by the UNAVCO-PBO station P494 during the Baja California, Mexico earthquake (Mw 7.2, 4 April 2010, 22:40:42 UTC; GPS Time–UTC = 15 s).

[52] The earthquake signature was clearly evident in the time series of the 3D velocities (BRD-S solution), which were compared to those derived from the complete variometric model using the best quality products supplied by IGS (PRE solution). The agreement of the two solutions (in terms of the standard deviations of the 3D velocity differences) was within 15 mm/s in the horizontal and 30 mm/s in height (Table 3), a slightly worse outcome than that obtained previously but still useful for recovering waveforms and coseismic displacements for a few centimeters in accuracy.

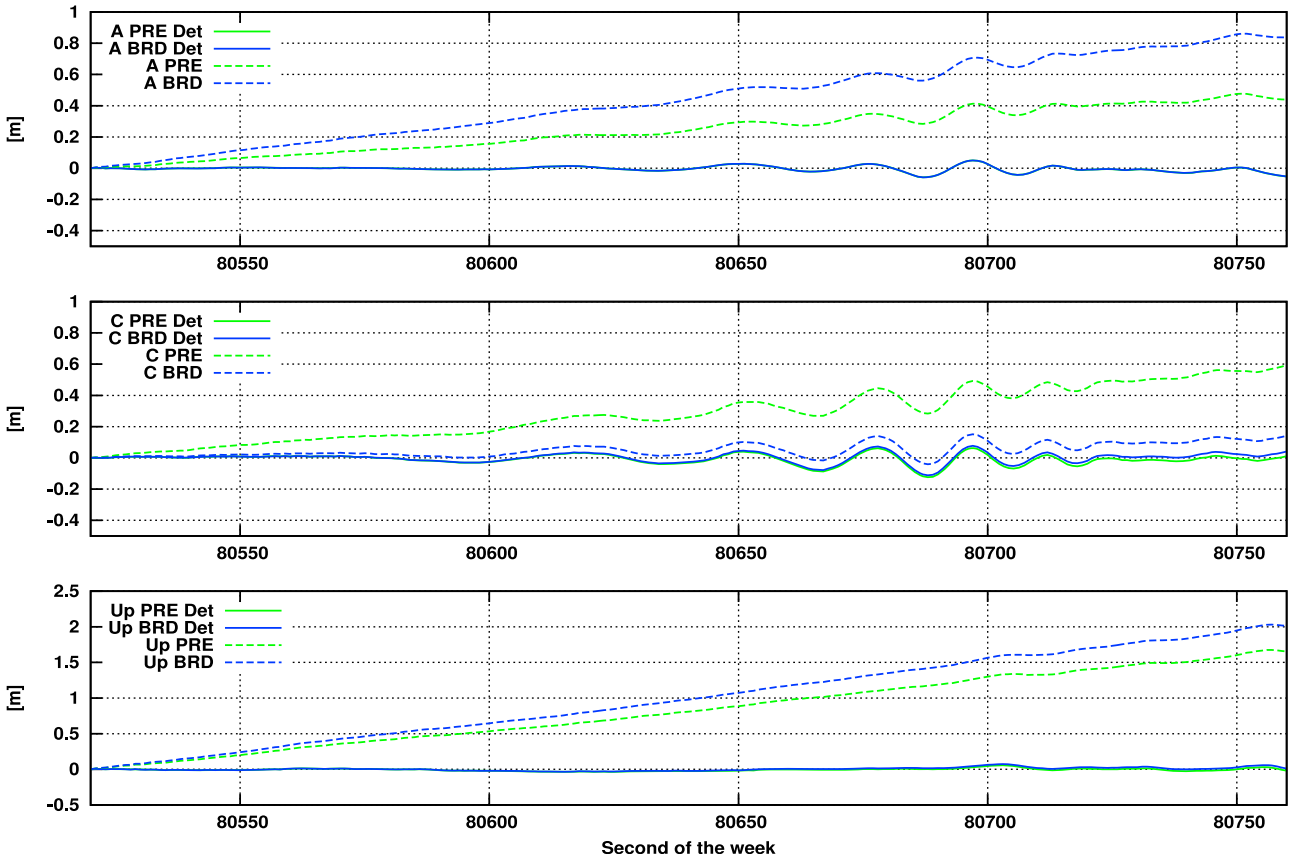

Figure 7. BREW coseismic displacements (along (A) and perpendicular (C) to the epicenter direction) obtained by integrating the estimated 3D velocities using broadcast products (BRD solution), and the best quality products supplied by IGS (PRE solution) before (dashed lines) and after (continuous lines) trend removal; 240 s interval 22:22:00–22:26:00 on 3 November 2002, GPS time. Direct comparison with the waveforms and coseismic displacements recovered by Jan Kouba [*Kouba*, 2003].

[53] In the final step, the 3D velocities were integrated and detrended (Figure 10), and compared with the solution presented by *UNAVCO* [2010]. Agreement in the horizontal components was at a level of a few centimeters if the waveforms minima and maxima were considered (Figure 11) (the vertical component comparison is not shown due to the higher noise of the solution and the much smaller waveform amplitude).

6. Conclusions and Prospects

[54] Here, we proposed a new approach for estimating coseismic displacements in the global reference frame in real time, based on a single GPS station technique that is able to overcome some of the difficulties displayed using presently adopted approaches for GPS seismology.

[55] Our approach (named VADASE) is based upon a so-called "variometric" solution, and only requires the standard GPS broadcast products (orbits and clocks), which are ancillary information routinely available in real time, and the observations collected by a unique, stand-alone, dual-frequency GPS receiver.

[56] The approach is based upon the time single-differences of the carrier phase observations collected at a high-rate (1 Hz or more) by a unique, stand-alone, receiver and the standard GPS broadcast products (orbits and clocks). The time series of the 3D velocities are, at first, estimated; then, they are integrated over the interval (limited to a few minutes) when the earthquake occurs. Estimation biases, due to a possible mismodeling of different intervening effects (such as multipath, residual clock errors, orbit errors, and atmospheric errors) accumulate over time and display their signature as a trend in coseismic displacements. The trend can be considered linear and easily removed at least for short intervals. Therefore, waveforms and coseismic displacements can be recovered, provided that the collected observations are continuous.

[57] After proving the functionality of a complete model, by using the best quality products supplied by IGS (PRE solution), as well as the standard GPS broadcast products (orbits and clocks) (BRD solution), the approach proved to be effective even when using a simplified model with standard information available in real time (GPS broadcast products, BRD-S solution).

[58] We tested VADASE on simulated and real data that are publicly available on the Web. Most of the significant results were obtained by considering data collected at a rate of 1 Hz from the IGS station BREW during the Denali Fault, Alaska earthquake (Mw 7.9, 3 November 2002, 22:12:41 UTC), and at a rate of 5 Hz with some stations

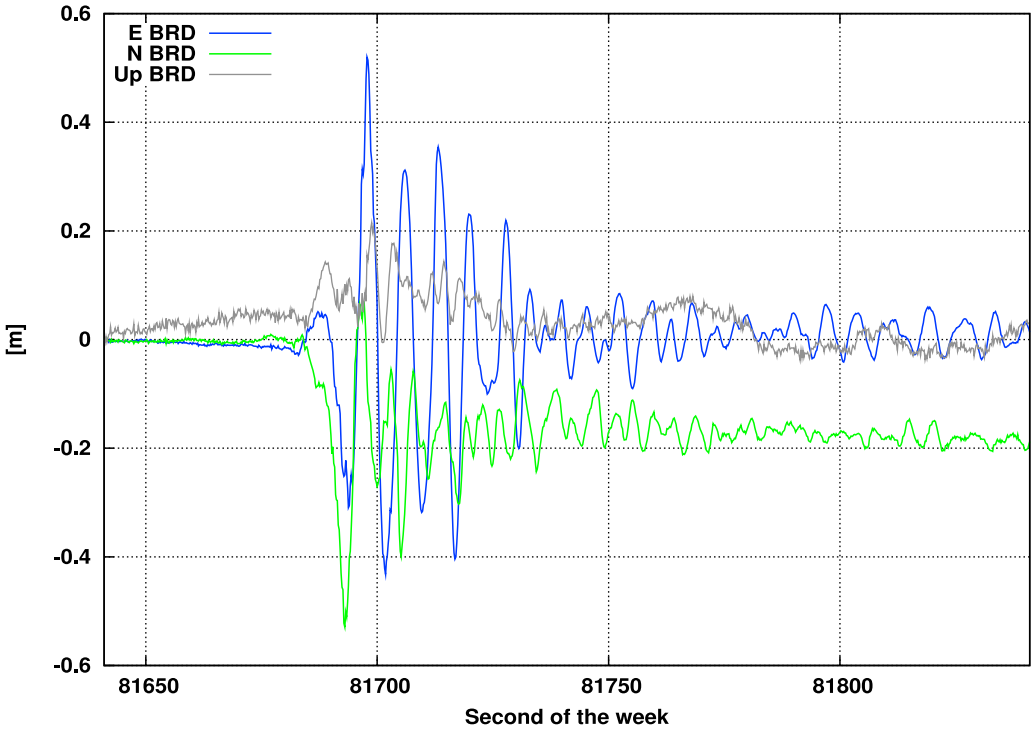

Figure 8. P496 coseismic displacements obtained by integrating the estimated 3D velocities (after trend removal) using broadcast products (BRD solution); 200 s interval 22:40:40–22:44:00 on 4 April 2010, GPS time. A direct comparison with coseismic displacements recovered by Kristine Larson at the University of Colorado at Boulder (http://www.unavco.org/voce/viewtopic.php?f = 48&t = 1214&sid = 992589027c26d02d4b30b15d6eea80a5#p2222).

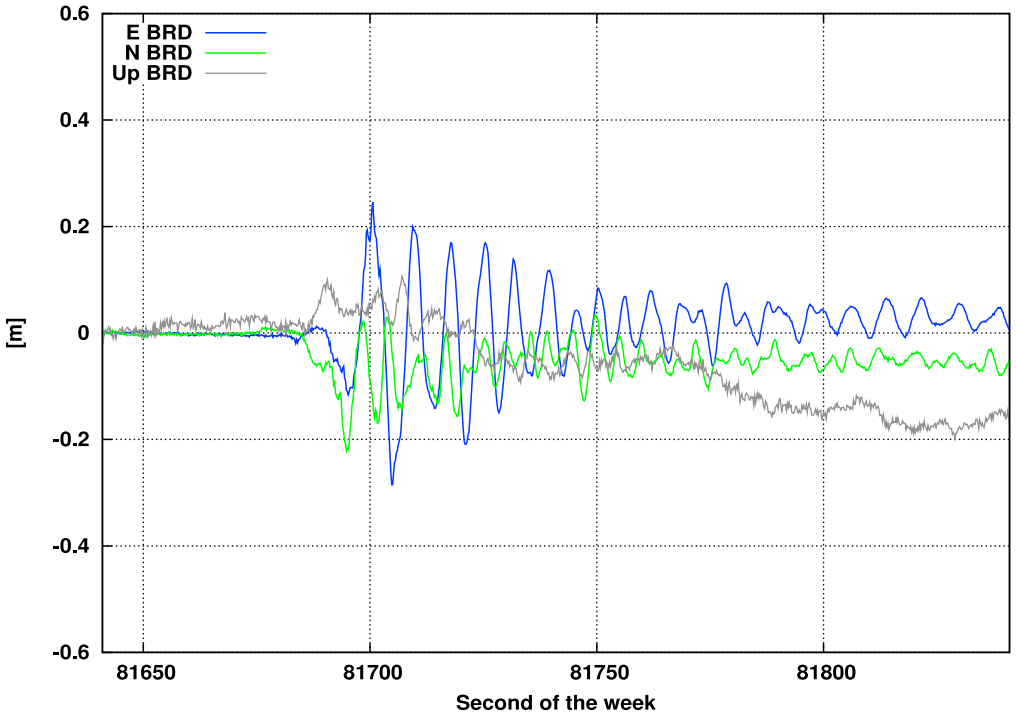

Figure 9. P744 coseismic displacements obtained by integrating the estimated 3D velocities (after trend removal) using broadcast products (BRD solution); 200 s interval 22:40:40–22:44:00 on 4 April 2010, GPS time. A direct comparison with coseismic displacements recovered by Kristine Larson at the University of Colorado at Boulder (http://www.unavco.org/voce/viewtopic.php?f = 48&t = 1214&sid = 992589027c26d02d4b30b15d6eea80a5#p2222).

Table 3. P494–PRE Versus BRD-S Estimated 3D Velocities[a]

	BRD-S – PRE [m/s]
E	0.0075
N	0.0115
Up	0.0310

[a]P494 comparisons between estimated 3D velocities using GPS broadcast products with the simplified model (BRD-S solution) and the best quality products supplied by IGS with the complete model (PRE solution); 220 s interval, 22:40:20–22:44:00, 4 April 2010, GPS time.

included in the UNAVCO-Plate Boundary Observatory network and the California Real Time Network (CRTN) during the Baja, California-Mexico earthquake (Mw 7.2, 4 April 2010, 22:40:42 UTC).

[59] The estimated displacements and waveforms displayed good agreement, at a level of a few centimeters, with previous analyses carried out on the same data set using other strategies (for example, the well-known Precise Point Positioning and Instantaneous Positioning approaches).

[60] In principle the VADASE algorithm can be embedded into a GPS receiver firmware. Considering the recommendation for achieving 1 cm real-time GNSS displacement accuracy in the global reference frame within the three minutes following an earthquake, the approach seems suited for use in tsunami warning systems.

[61] Here, it is also useful to outline two significant added values when using GPS receivers to estimate coseismic displacements and seismic waveforms, in addition to standard seismometers.

[62] 1. The seismic moment (and the moment magnitude (M_w)) may be retrieved without the problem of saturation, which commonly affects seismometers close to the epicenter during large earthquakes.

[63] 2. GPS receivers may work in "twin-fashion" mode (that is at a low and at a high rate), which enables estimations for both of the low deformations (pre-seismic and post-seismic) and for coseismic displacements and waveforms.

[64] The major drawback of the approach is the mandatory request for data continuity in order to enable velocity integration over the interval of interest. In this respect, the joint processing of GPS and GLObal'naja Navigacionnaja Sputnikovaja Sistema (GLONASS) dual frequency observations increases the number of potentially available satellites, and, as a result, increases the reliability of our approach.

[65] In the end, we need to sketch out some issues, as follows, which could be addressed in the near-future in order to better assess the variometric approach's potential and to possibly enlarge its applications: (1) the previously mentioned joint processing of GPS and GLONASS dual frequency observations; (2) a comparison with the corresponding solutions derived from different strategies on a

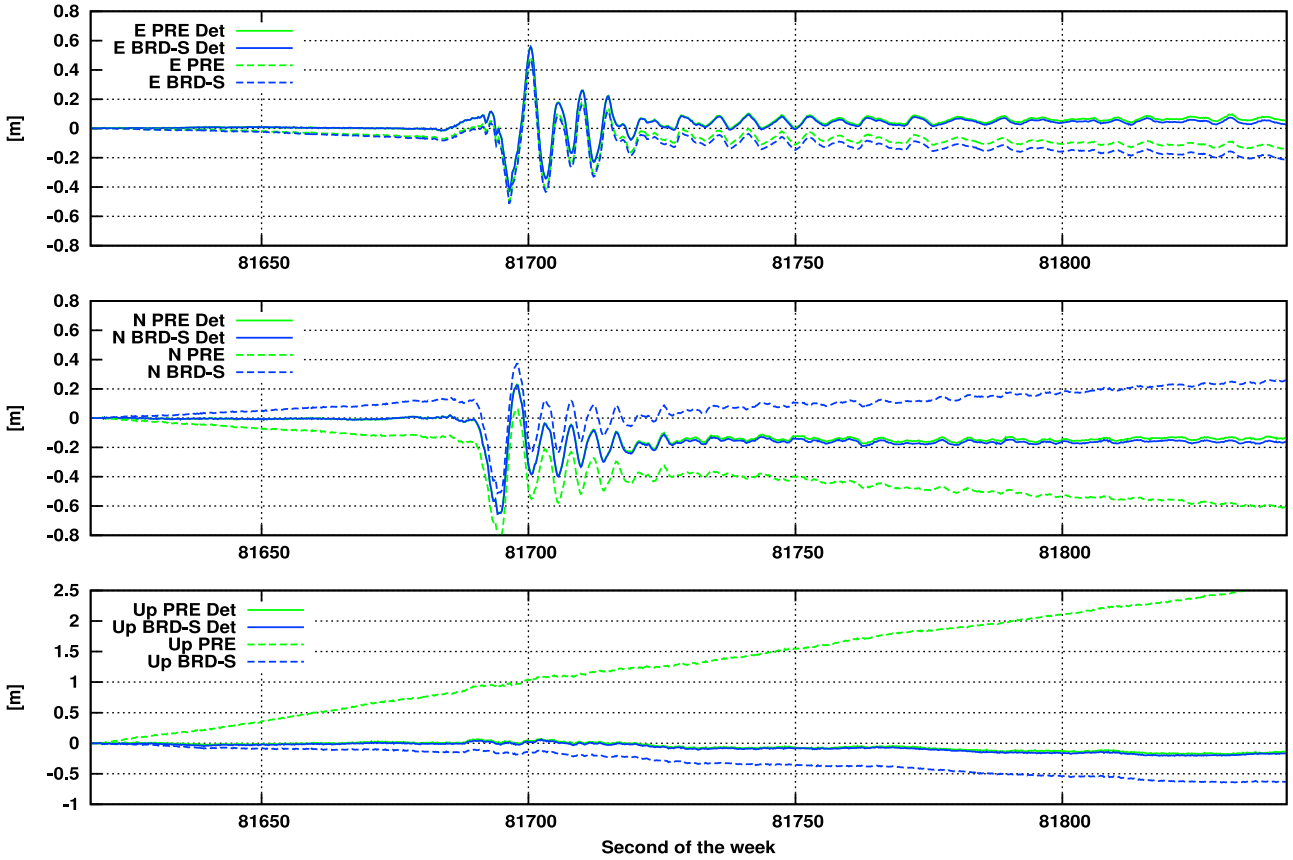

Figure 10. P494 coseismic displacements obtained by integrating the estimated 3D velocities using broadcast products with the simplified model (BRD-S solution) and the best quality products supplied by IGS (PRE solution) before (dashed lines) and after (continuous lines) trend removal; 220 s interval 22:40:20–22:44:00 on 4 April 2010, GPS time.

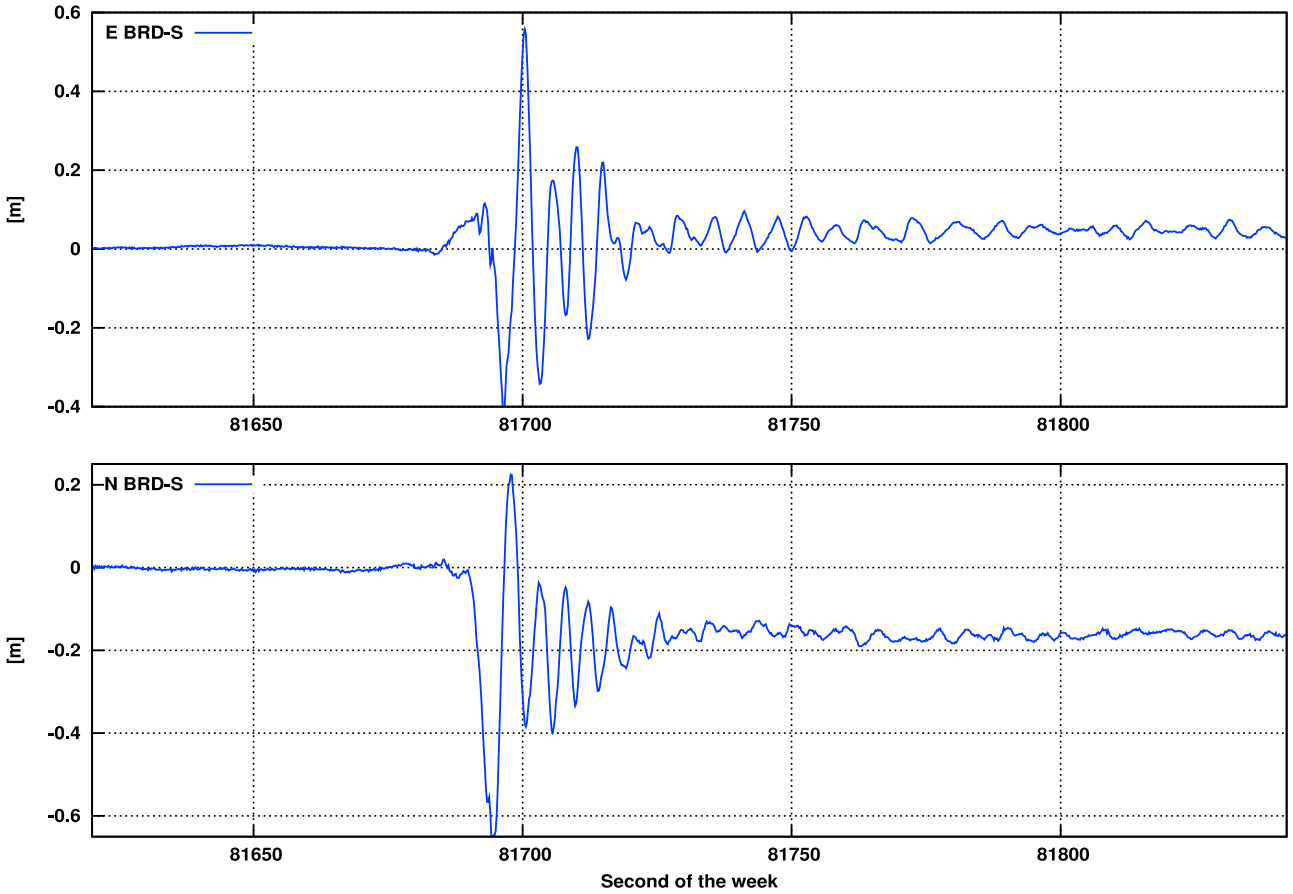

Figure 11. P494 coseismic displacements obtained by integrating the estimated 3D velocities (after trend removal) using broadcast products with the simplified model (BRD-S solution); 220 s interval 22:40:20–22:44:00 on 4 April 2010, GPS time. A direct comparison with the waveforms and coseismic displacements recovered by Yehuda Bock at UCSD and Sharon Kedar at JPL (http://www.unavco.org/research_science/science_highlights/2010/M7.2-Baja-SesimicGPSDisplacements.pdf).

larger sample; (3) the application of single frequency and low-cost phase receivers; (4) a comparison with other high-rate instruments, such as ground radar interferometers, on a local scale (for example, for structural purposes); and (5) the application of possibly more refined detrending strategies.

[66] **Acknowledgments.** We recognize the fundamental role of the IGS, the UNAVCO-Plate Boundary Observatory network, and the California Real Time Network for delivering high-rate GNSS data in near real time. We also thank the Editor, the Associate Editor, and two anonymous reviewers for their careful review, their appreciation of our work, and very useful remarks and suggestions, which certainly contributed to improving the manuscript. The variometric approach as presented in this paper is the subject of a pending patent. VADASE was awarded the DLR Special Topic Prize on 18 October 2010 and the first European Satellite Navigation Competition Audience Award on 16 November 2010, under the framework of the European Satellite Navigation Competition 2010 (http://www.galileo-masters.eu/).

References

Berg, H. (1948), *Allgemeine Meteorologie*, Dümmler's Verlag, Bonn, Germany.

Bilich, A., K. Larson, and J. F. Cassidy (2008), GPS seismology: Application to the 2002 M*w* 7.9 Denali Fault Earthquake, *Bull. Seismol. Soc. Am.*, *98*(2), 593–606, doi:10.1785/0120070096.

Blewitt, G., C. Kreemer, W. C. Hammond, H. P. Plag, S. Stein, and E. Okal (2006), Rapid determination of earthquake magnitude using GPS for tsunami warning systems, *Geophys. Res. Lett.*, *33*, L11309, doi:10.1029/2006GL026145.

Blewitt, G., W. C. Hammond, C. Kreemer, H. P. Plag, S. Stein, and E. Okal (2009), GPS for real-time earthquake source determination and tsunami warning systems, *J. Geod.*, *83*, 335–343, doi:10.1007/s00190-008-0262-5.

Bock, Y., and J. F. Genrich (2006), Instantaneous geodetic positioning with 10–50 Hz GPS measurements: Noise characteristics and implications for monitoring networks, *J. Geophys. Res.*, *111*, B03403, doi:10.1029/2005JB003617.

Bock, Y., et al. (1993), Detection of crustal deformation from the Landers earthquake sequence using continuos geodetic measurements, *Nature*, *361*, 337–340, doi:10.1038/361337a0.

Bock, Y., R. M. Nikolaidis, and P. de Jonge (2000), Instantaneous geodetic positioning at medium distances with the Global Positioning System, *J. Geophys. Res.*, *105*(B12), 28,223–28,253, doi:10.1029/2000JB900268.

Bock, Y., L. Prawirodirdjo, and T. I. Melbourne (2004), Detection of arbitrarily large dynamic ground motions with a dense high-rate GPS network, *Geophys. Res. Lett.*, *31*, L06604, doi:10.1029/2003GL019150.

Choi, K., A. Bilich, K. M. Larson, and P. Axelrad (2004), Modified sidereal filtering: Implications for high-rate GPS positioning, *Geophys. Res. Lett.*, *31*, L22608, doi:10.1029/2004GL021621.

Dach, R., H. Hugentobler, P. Fridez, and M. Meindl (2007), Bernese GPS Software Version 5.0, user's manual, Astron. Inst., Univ. of Bern, Bern.

Dow, J. M., R. E. Neilan, and C. Rizos (2009), The International GNSS Service in a changing landscape of Global Navigation Satellite Systems, *J. Geod.*, *83*, 191–198, doi:10.1007/s00190-008-0300-3.

Hofmann-Wellenhof, B., H. Lichtenegger, and E. Wasle (2008), *Global Navigation Satellite Systems*, Springer, NewYork.

Kouba, J. (2003), Measuring seismic waves induced by large earthquakes with GPS, *Stud. Geophys. Geod.*, *47*(4), 741–755, doi:10.1023/A:1026390618355.

Kouba, J. (2005), A possible detection of the 26 December 2004 Great Sumatra-Andaman Islands Earthquake with solution products of the International GNSS Service, *Stud. Geophys. Geod.*, *49*, 463–483, doi:10.1007/s11200-005-0022-4.

Langbein, J., and Y. Bock (2004), High-rate real-time GPS network at Parkfield: Utility for detecting fault slip and seismic displacements, *Geophys. Res. Lett.*, *31*, L15S20, doi:10.1029/2003GL019408.

Larson, K. (2009), GPS seismology, *J. Geod.*, *83*, 227–233, doi:10.1007/s00190-008-0233-x.

Larson, K., and S. Miyazaki (2008), Resolving static offsets from high-rate GPS data: The 2003 Tokachi-oki earthquake, *Earth Planets Space*, *60*, 801–808.

Larson, K., P. Bodin, and J. Gomberg (2003), Using 1-Hz GPS data to measure deformations caused by the Denali Fault earthquake, *Science*, *300*, doi:10.1126/science.1084531.

Larson, K., A. Bilich, and P. Axelrad (2007), Improving the precision of high-rate GPS, *J. Geophys. Res.*, *112*, B05422, doi:10.1029/2006JB004367.

McCarthy, D. D., and G. Petit (Eds.) (2004), *IERS Conventions (2003), IERS Tech. Note 32*, 127 pp., Bundesamts fur Kartographie und Geod., Frankfurt am Maim, Germany. [Available at http://www.iers.org/IERS/EN/Publications/TechnicalNotes/tn32.html.]

Miyazaki, S., and K. Larson (2008), Coseismic and early postseismic slip for the 2003 Tokachi-oki earthquake sequence inferred from GPD data, *Geophys. Res. Lett.*, *35*, L04302, doi:10.1029/2007GL032309.

Plag, H. P., G. Blewitt, C. Kreemer, and W. C. Hammond (2005), Solid earth deformations induced by the Sumatra earthquakes of 2004–2005: GPS detection of co-seismic displacements and tsunami-induced loading, *IEEE Trans. Electron. Dev.*, *23*, 648–650.

Saastamoinen, J. (1972), Atmospheric correction for the troposphere and stratosphere in radio ranging of satellites, in *The Use of Artificial Satellites for Geodesy*, *Geophys. Monogr. Ser.*, vol. 15, edited by S. W. Henriksen, A. Mancini, and B. H. Chovitz, pp. 247–251, AGU, Washington, D. C.

G. Colosimo, M. Crespi, and A. Mazzoni, DICEA–Area di Geodesia e Geomatica, Università di Roma "La Sapienza," Via Eudossiana 18, Rome I-00184, Italy. (mattia.crespi@uniroma1.it)